Article

Closo-alanes (AlH, AlH, 4 □ *n* □ 8): A New Chapter in Aluminum Hydride Chemistry

A. Grubisic, X. Li, S. T. Stokes, J. Cordes, G. F. Gantefr, K. H. Bowen, B. Kiran, P. Jena, R. Burgert, and H. Schnckel

J. Am. Chem. Soc., **2007**, 129 (18), 5969-5975• DOI: 10.1021/ja0700404 • Publication Date (Web): 17 April 2007

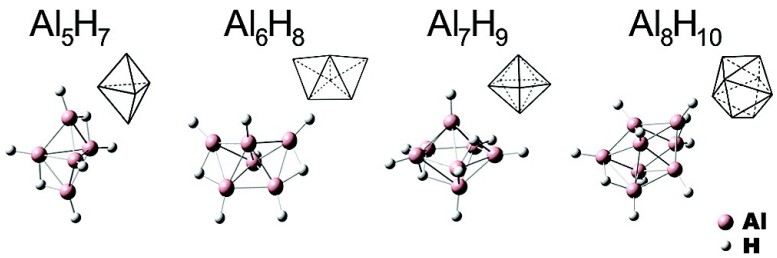

More About This Article

Additional resources and features associated with this article are available within the HTML version:

- Supporting Information
- Links to the 6 articles that cite this article, as of the time of this article download
- Access to high resolution figures
- Links to articles and content related to this article
- Copyright permission to reproduce figures and/or text from this article

View the Full Text HTML

J|A|C|S
ARTICLES
Published on Web 04/17/2007

Closo-alanes (Al_4H_4, Al_nH_{n+2}, $4 \leq n \leq 8$): A New Chapter in Aluminum Hydride Chemistry

A. Grubisic,[†] X. Li,[†] S. T. Stokes,[†] J. Cordes,[‡] G. F. Ganteför,[‡,†] K. H. Bowen,[†,*] B. Kiran,[§] P. Jena,[§] R. Burgert,[||] and H. Schnöckel[||]

Contribution from the Departments of Chemistry and Materials Science, Johns Hopkins University, Baltimore, Maryland 21218, Department of Physics, University of Konstanz, 78457 Konstanz, Germany, Department of Physics, Virginia Commonwealth University, Richmond, Virginia 23284, and Institute of Inorganic Chemistry, University of Karlsruhe (TH), 76128 Karlsruhe, Germany

Received January 10, 2007; E-mail: kbowen@jhu.edu

Abstract: Anion photoelectron spectroscopy and density functional theory were employed to study aluminum hydride clusters, $Al_nH_m^-$ ($4 \leq n \leq 8$, $0 \leq m \leq 10$). Photoelectron spectra revealed that Al_4H_4, Al_4H_6, and a family of species with general formula Al_nH_{n+2} ($5 \leq n \leq 8$) have small adiabatic electron affinities and large HOMO−LUMO gaps (ranging from 0.5 to 1.9 eV) relative to those of their stoichiometric neighbors, implying their enhanced stabilities. Formulas reminiscent of boranes led us to investigate whether Wade's rules could be applied to alanes as well. DFT calculations showed that the Al_nH_{n+2} ($5 \leq n \leq 8$) family adopts *n*-vertex polyhedral closo-structures with two extra hydrogen atoms occupying opposite bridging positions in agreement with the Wade's ($n + 1$) rule. These can be viewed as aluminum versions of hypothetical diprotonated closo-borane dianions ($B_nH_n^{2-} + 2H^+$). In addition, Al_4H_4 assumes a closo-tetrahedral geometry, while Al_4H_6 takes on a distorted tetrahedral (D_{2d}) structure with two counter-positioned bridging hydrogen atoms and has the largest HOMO−LUMO gap (1.9 eV) of all the alanes we studied. All of these species can be understood in terms of underlying polyhedral skeletal electron pair theory (PSEPT) concepts. Although, the herein studied alanes do not have direct borane analogues, the ability to understand their structures in terms of the Wade−Mingos rules and the underlying PSEPT concepts suggests that they can be considered as borane analogues, thereby opening a new chapter in aluminum hydride chemistry.

1. Introduction

Few elements in the same group of the periodic table show such disparities in hydride chemistry as do the two lightest members of the main group III, aluminum and boron. Aluminum chemistry in general is overwhelmingly that of 0 and +3 oxidation states and the chemistry of aluminum hydrides is no exception. There are only a few known aluminum hydrides (alanes).[1] AlH_3 and Al_2H_6 molecules have been seen in cryogenic matrices[2,3] and perhaps the gas phase.[4] In the solid phase a polymeric alane, $(AlH_3)_n$ is known, as are AlH_4^- and AlH_6^{3-} in their alkali metal salts, the alanates, for example, $LiAlH_4$.[5] In molecular beams $Al_{13}H^-$ has been prepared[6,7] as well as several dissociative chemisorption products of $D_2 + Al_n^-$ interactions.[8]

Boron, on the other hand, is famous for its rich hydride chemistry,[9,10] where boron exhibits fractional oxidation states. Since the field opened in 1912 with preparation and characterization of the first boron hydrides (i.e., boranes),[11] attempts to explain the unusual variety of structural motifs seen in these compounds introduced several revolutionary ideas into the world of chemistry. Insufficient valence electrons in boron, that is, to satisfy the octet rule, led to the proposition of a three-centered-two-electron (3c-2e) bond.[12] Using this concept, an extension to molecular orbital (MO) theory was developed, known as the polyhedral skeletal electron pair theory (PSEPT) or simply Wade−Mingos rules.[13−15] It took into account the extensive experimental evidence that the most common building block of the known boranes is the {BH} fragment. By focusing on one such unit and the ways it connects with its neighbors the theory successfully explained the structures of most known boranes and even predicted the existence of some that were not discovered until later. The boron atom in the {BH} fragment is assumed to be sp-hybridized and allocates one sp orbital and

[†] Johns Hopkins University.
[‡] University of Konstanz.
[§] Virginia Commonwealth University.
[||] University of Karlsruhe (TH).

(1) Aldridge, S.; Downs, A. J. *Chem. Rev.* **2001**, *101* (11), 3305.
(2) Kurth, F. A.; Schnöckel, R. A. E. H.; Downs, A. J.; Pulham, C. R. *J. Chem. Soc.* **1993**, *16*, 1302.
(3) Andrews, L.; Wang, X. *Science* **2003**, *299* (5615), 2049.
(4) Breisacher, P.; Siegal, B. *J. Am. Chem. Soc.* **1964**, *86* (22), 5053.
(5) Wilkinson, F. A. C. a. G. *Advanced Inorganic Chemistry*, 2nd ed.; Interscience: New York, 1966.
(6) Rao, B. K.; Jena, P.; Burkart, S.; Ganteför, G.; Seifert, G. *Phys. Rev. Lett.* **2001**, *86* (4), 692.
(7) Burkart, S.; Blessing, N.; Klipp, B.; Miller, J.; Ganteför, G.; Seifert, G. *Chem. Phys. Lett.* **1999**, *301* (5−6), 546.
(8) Cui, L.-F.; Li, X.; Wang, L.-S. *J. Chem. Phys.* **2006**, *124* (5), 054308.
(9) Lipscomb, W. N. *Boron Hydrides*. W. A. Benjamin: New York, 1963.
(10) Greenwood, N. N. A. E. *Chemistry of the Elements*, 2nd ed.; Elsevier Science: Amsterdam, The Netherlands, 1997.
(11) Stock, A.; Massenez, C. *Ber. Dtsch. Chem. Ges.* **1912**, *45* (3), 3539.
(12) Longuet-Higgins, H. C. *J. Chim. Phys. Phys.-Chim. Biol.* **1949**, *46*, 268.
(13) Mingos, D. M. P. *Nat.-Phys. Sci.* **1972**, *236* (68), 99.
(14) Wade, K. *Adv. Inorg. Chem. Radiochem.* **1976**, *18*, 1.
(15) Williams, R. E. *Chem. Rev.* **1992**, *92* (2), 177.

one electron for forming a traditional, localized bond with the H atom (i.e., exo B−H bond). The remaining three, unfilled orbitals (1 sp + 2 p's) plus two electrons then become the basis of the cluster skeletal bonding. Concentrating on these skeletal orbitals, the PSEP theory shows that in structures based on *n*-vertex polyhedra, most commonly seen in boranes, a set of $(n + 1)$ bonding molecular orbitals is generated. Sufficient electrons, that is, $n + 1$ electron pairs, to fill the skeletal bonding orbitals, stabilizes such a framework. Turning the argument around, depending on the number of valence electrons that are available for skeletal bonding (those not involved in *exo*-bonds), the framework adopts geometries built on different *n*-vertex polyhedra.

A set of earlier-developed, empirically derived electron counting rules, known as the Wade's rules,[14,16] allows one to quickly apply the conclusions of the PSEPT without considering the details of the underlying MO picture. The most familiar Wade's rule applies to *closo*-boranates of stoichiometry, $B_nH_n^{2-}$ which contain $(2n + 1)$ valence electron pairs. Of these, *n* pairs are required by the B−H *exo*-bonds, leaving $n + 1$ electron pairs for skeletal bonding. Remembering that according to PSEPT an *n*-vertex polyhedral structure contains $n + 1$ bonding orbitals that can accommodate all the available skeletal electrons, the Wade's $(n + 1)$ rule can be formulated: a borane with $n + 1$ electron pairs for skeletal bonding will have a structure based on a closed *n*-vertex polyhedron; for example, $B_{12}H_{12}^{2-}$ is an icosahedron. The rule, however, holds only for $n > 4$. The well-known tetrahedral exception to the Wade's $(n + 1)$ rule[17,18] occurs because of the nature of the underlying MO diagram in the $n = 4$ case.

Triumphant in explaining the structures of molecules for which they were initially developed, the generality of the PSEPT approach enables the Wade's rules to transcend the realm of boron hydrides and helps predict the structures of such diverse systems as carboranes, metalloboranes, metallo-carbonyls, metal-hydrocarbon-π-systems,[14,15] mixed metal clusters, and Zintl ions.[19] Despite their widespread applicability in inorganic cluster chemistry, however, similar structures for aluminum hydrides had not been observed, even though aluminum and boron have equal numbers of valence orbitals and electrons, and this would seem to allow the application of Wade's rules to alanes as well as to boranes.

In this paper, we present results of a combined anion photoelectron spectroscopic and theoretical study on aluminum hydrides that reveals the existence of several previously unknown alane species with enhanced stability, marking the opening of a new chapter in aluminum hydride chemistry. Aluminum hydride cluster anions, $Al_nH_m^-$, containing as many as 10 hydrogen atoms per aluminum cluster were generated in a pulsed arc cluster ionization source (PACIS).[20] The anion photoelectron spectra of $(Al_nH_{n+2})^-$, $4 \le n \le 8$, and of $Al_4H_4^-$ showed large HOMO−LUMO gaps (0.5−1.9 eV) and low adiabatic electron affinities (EA_a) for their corresponding neutral species. This combination usually indicates enhanced stabilities. (For example, the HOMO−LUMO gaps for C_{60} and KAl_{13}, are ~1.7 and 1.3 eV, respectively).[21,22] By finding structures that reproduce the observed photoelectron spectra, theoretical calculations were able to show that all of these structures conform to PSEPT concepts and to a large extent follow the Wade's rules. In particular, we show that Al_nH_{n+2} $(5 \le n \le 8)$ can be treated as $Al_nH_n^{2-} + 2H^+$ in analogy with the closo-boranates of general formula, $B_nH_n^{2-}$, even though diprotonated forms of closo-borane dianions have not been observed experimentally. In addition, we show that the $n = 4$ species Al_4H_4 and Al_4H_6 adopt tetrahedral and distorted tetrahedral structures, respectively, thus extending the family of closo-alanes. Finally, it is worthwhile noting that the derivatives of Al_4H_4 have already been synthesized[23,24] and that both Al_4H_4 and Al_4H_6 have borane-related analogues, B_4R_4 (R= ^{t}Bu, Cl, Br, $CH_2{}^t$Bu)[25] and $B_4H_2R_4$,[26] respectively. Thus, the aluminum hydride species presented here can be viewed as borane analogues.

2. Methods

2.1. Experimental. Anion photoelectron spectroscopy is conducted by crossing a beam of mass-selected negative ions with a fixed-frequency photon beam and energy-analyzing the resultant photodetached electrons. The photodetachment process is governed by the energy-conserving relationship, $h\nu = EBE + EKE$, where $h\nu$ is the photon energy, EBE is the electron binding energy, and EKE is the electron kinetic energy. The main information obtained is the electronic energy spectrum of the anion's corresponding neutral at the structure of the anion. Thus, even though these experiments are performed on negative ions, their results pertain to their neutral counterparts as well.

Our apparatus has been described previously.[27] Briefly, the apparatus consists of an ion source, a linear time-of-flight mass selector (TOF-MS), a Nd:YAG photodetachment laser, and a magnetic bottle photoelectron spectrometer (MB-PES). The instrumental resolution of the MB-PES is ~35 meV at 1 eV EKE. The third (355 nm, 3.496 eV) and fourth (266 nm, 4.661 eV) harmonic of a Nd:YAG were used to photodetach the cluster anions of interest. Photoelectron spectra were calibrated against the known atomic lines of Cu^-. In this study, aluminum hydride anions were generated with a pulsed arc cluster ionization source (PACIS). Ganteför et al.[7] first realized the value of the PACIS for studying aluminum cluster anion interactions with hydrogen, when they employed it in their study of $Al_{13}H^-$. Although a detailed description of the source is given elsewhere,[20] a brief summary will be given here. About 200 psi of UHP hydrogen gas is back-filled into a region between an anode and a grounded aluminum sample cathode. Then, a 30−40 μs long 100 V pulse is applied to the anode causing a discharge between the electrodes in which hydrogen gas partially dissociates (generating a momentarily high concentration of H atoms) and aluminum atoms are vaporized. About 50 psi of helium gas flushes the hydrogen−aluminum plasma mix down a 20 cm flow tube, where it reacts, cools, and forms clusters. The source was operated at 10 Hz repetition rate.

2.2. Theoretical. The equilibrium geometries of the species studied in this work were calculated using the self-consistent linear combination of atomic orbitals−molecular orbital (SCF-LCAO-MO) method. The TZVP basis set was used for the atomic orbitals of Al and H, and the total energies were computed using the density functional with the

(16) Wade, K. *J. Chem. Soc. D.* **1971**, *15*, 792.
(17) Stone, A. J.; Alderton, M. J. *J. Inorg. Chem.* **1982**, *21*, 2297.
(18) Fowler, P. W. *Polyhedron* **1985**, *4*, 2051.
(19) Lauher, J. W. *J. Am. Chem. Soc.* **1978**, *100*, 5303.
(20) Siekmann, H. R.; Lueder, C.; Faehrmann, J.; Lutz, H. O.; Meiwes-Broer, K. H. *Z. Phys. D: At., Mol. Clusters* **1991**, *20* (1−4), 417.
(21) Yang, S. H.; Pettiette, C. L.; Conceicao, J.; Cheshnovsky, O.; Smalley, R. E. *Chem. Phys. Lett.* **1987**, *139*, 233.
(22) Zheng, W.-J.; Thomas, O. C.; Lippa, T. P.; Xu, S.-J.; Bowen, K. H. *J. Chem. Phys.* **2006**, *124*, 144304.
(23) Roesky, H. W. *Inorg. Chem.* **2004**, *43*, 7284.
(24) Balakrishnarajan, M. M.; Hoffmann, R. *J. Am. Chem. Soc.* **2004**, *126*, 13119.
(25) Neu, A.; Mennekes, T.; Paetzold, P.; Englert, U.; Hofmann, M.; Schleyer, P. v. R. *Inorg. Chim. Acta* **1999**, *289*, 58.
(26) Neu, A.; Mennekes, T.; Englert, U.; Paetzold, P.; Hofmann, M.; Schleyer, P. v. R. *Angew. Chem., Int. Ed. Engl.* **1997**, *36* (19), 2117.
(27) Gerhards, M.; Thomas, O. C.; Nilles, J. M.; Zheng, W.-J.; Bowen, K. H. *J. Chem. Phys.* **2002**, *116* (23), 10247.

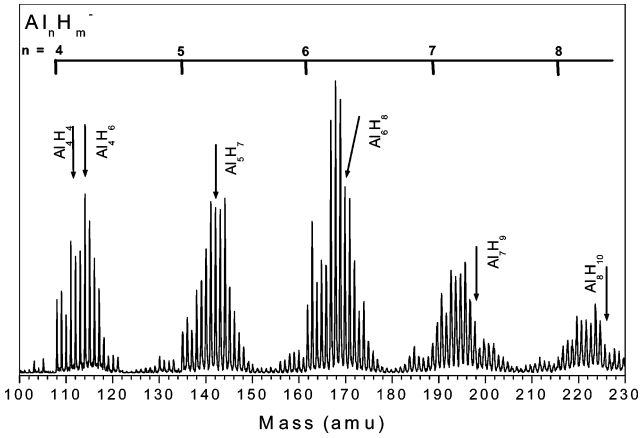

Figure 1. Typical mass spectrum of $Al_nH_m^-$ clusters generated in PACIS. Arrows mark the peaks corresponding to specific closo-alane species.

PW91 as an exchange and correlation functional. The geometries were optimized by using different initial configurations without any symmetry restrictions. Frequency calculations on the optimized geometries were done to establish the nature of the stationary point, and all the structures were found to have stable minima (all positive vibrations) on the potential energy surface. To compute HOMO−LUMO gaps, vertical excitation energies were calculated using the TDDFT method. All calculations were done with Gaussian 03 software.[28]

3. Results and Discussion

A typical mass spectrum of $Al_nH_m^-$ clusters produced in our PACIS source is shown in Figure 1. Typically, 10 or more hydrogen atoms had attached to each aluminum cluster size, *n*. Prominent peaks in the hydride anion distribution are associated with special stability of those species and usually occur among the smaller clusters ($n \le 6$). High ion intensity was due either to enhanced stability of the ion, such as closed shell Al_6H^- or to the stability of the underlying neutral from which the ions are formed, for example, Al_4H_6.[29]

While we collected photoelectron spectra for many $Al_nH_m^-$ stoichiometries, here we present data only for those of $Al_nH_{n+2}^-$ ($5 \le n \le 8$) and $Al_4H_m^-$ ($3 \le m \le 7$) series. In what follows, we focus on each alane species separately from a theoretical as well as an experimental point of view. In particular, two quantities will be of special interest, the adiabatic electron affinity, EA_a, and the HOMO−LUMO gap of the neutral species. Both were experimentally determined from photoelectron spectra of their corresponding anions, and these quantities serve as benchmark values for the theoretical determination of their structures.

Peaks in photoelectron spectra arise because of transitions from the ground electronic state of a particular anion to the ground and excited electronic states of its corresponding neutral. The lowest electron binding energy (EBE) peak is due to the transition between the ground state of the anion and that of its corresponding neutral, thus providing a measurement of the value of EA_a. The threshold region of the lowest EBE peak in the photoelectron spectrum was utilized throughout this paper to estimate the value of EA_a. The EBE of the intensity maximum in the lowest EBE peak defines the vertical detachment energy

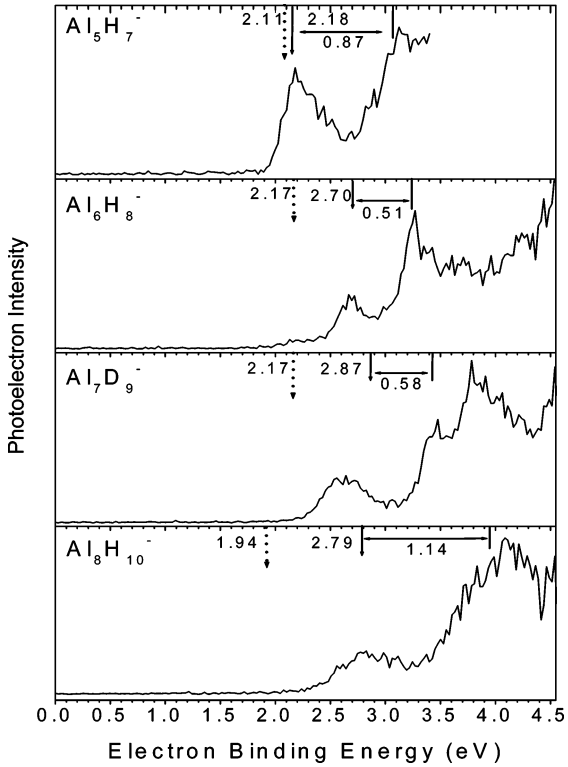

Figure 2. Photoelectron spectra of $Al_nH_{n+2}^-$ ($5 \le n \le 8$). Arrows indicate theoretically calculated values for EA_a (dotted,vertical), VDE (solid, vertical), and HOMO−LUMO gap (solid, horizontal). All spectra were recorded with 4.661 eV photons except the $n = 5$ case for which 3.496 eV photons were utilized.

(VDE), and it reflects the Franck−Condon overlap between vibrational wave-functions of the anion and its corresponding neutral at the geometry of the anion.

Of most interest in this paper is the splitting between the two lowest EBE features. Within Koopmans' approximation this energy difference is interpreted as the HOMO−LUMO gap of the anion's corresponding neutral. An electronically stable, closed-shell neutral molecule or cluster has a low-lying HOMO associated with stabilization owing to closing of its outermost shell. Thus, the extra electron in its corresponding anion must go into the relatively high-lying LUMO. For these reasons, a large splitting in tandem with a small electron affinity signals substantial stability in the anion's neutral counterpart. The HOMO−LUMO gap for each alane was estimated as the difference between maxima of the two lowest EBE peaks. The absence of such a spectral splitting indicates the lack of a substantial HOMO−LUMO gap.

3.1. Closo-alanes: Al_nH_{n+2} ($5 \le n \le 8$). An analysis of the photoelectron spectra of $Al_nH_m^-$ showed an emerging pattern where significant HOMO−LUMO gaps were observed for species having general formula Al_nH_{n+2}. Their anion photoelectron spectra are shown in Figure 2. Stoichiometries reminiscent of hypothetical diprotonated closo-borane dianions (B_nH_{n+2}) led us to investigate whether these species could be understood in terms of Wade's rules. Assuming two extra hydrogen atoms become an integral part of the aluminum cage by forming 3c-2e bonds with two neighboring aluminum atoms, their two electrons can be thought of as having been donated to skeletal bonding. We can then formally treat Al_nH_{n+2} as $Al_nH_n^{2-} + 2H^+$. Being prototypical model compounds for

(28) Frisch, M. J.; et al. *Gaussian 03*, revision C.02; Gaussian, Inc.: Pittsburgh, PA, 2004.
(29) Li, X.; Grubisic, A.; Stokes, S. T.; Cordes, J.; Ganteför, G. F.; Bowen, K. H.; Kiran, B.; Willis, M.; Jena, P.; Burgert. R.; Schnöckel, H. *Science* **2007**, *315*, 356.

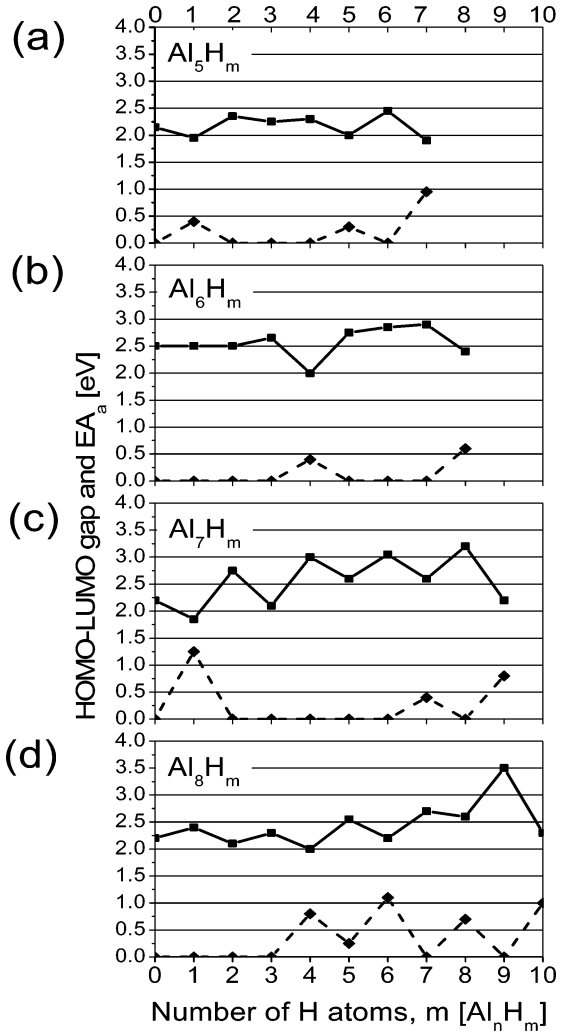

Figure 3. HOMO−LUMO gaps (dashed) and EA_a values (solid) for clusters of the (a) Al_5H_m, (b) Al_6H_m, (c) Al_7H_m, (d) Al_8H_m series versus the number of hydrogen atoms, *m*.

Wade's ($n + 1$) rule, the geometries of all these species are predicted to be those of *n*-vertex polyhedra. Note that according to Wade's rules, the two extra hydrogen atoms are predicted to bind via bridging/facile sites, but they are not assigned to a specific position on the aluminum cage. Because of the many possible arrangements of the two bridging hydrogen atoms relative to each other, there are numerous low-energy isomers that differ only slightly in energy. Since they usually also exhibit similar photoelectron signatures, we rely on our calculations to sort out the specific ground-state isomeric structure of the respective species. This limitation is inherent in all Al_nH_{n+2} ($5 \leq n \leq 8$) species that we studied.

3.1.1. Pentaalane ($n + 2 = 7$): Al_5H_7. The photoelectron spectrum of $Al_5H_7^-$ (see Figure 2) contains two prominent features, located at 2.20 ± 0.05 and 3.15 ± 0.10 eV. Their separation of 0.95 eV is interpreted as the HOMO−LUMO gap of the corresponding neutral, Al_5H_7. The values of EA_a and HOMO−LUMO for all members of the Al_5H_m series are plotted in Figure 3a. With a large HOMO−LUMO gap and a low value of EA_a, Al_5H_7 stands out among its neighbors. Our theoretical calculations reproduce the main features of the spectrum very well and are marked in Figure 2 as well as tabulated in Table 1. The structure of the neutral ground state (Figure 4a) was determined to have a slightly distorted Al_5H_5 trigonal bipyramidal core with two bridging hydrogen atoms in agreement with predictions of the Wade's ($n + 1$) rule. The two extra hydrogen atoms position themselves onto opposite edges of the polyhedron, probably in an effort to minimize steric hindrance. Also, note that Al_5H_6, the cluster with one hydrogen atom less than Al_5H_7, displays the highest electron affinity value in the series. This observation is generalized among the trends seen in Figure 3 and will be further discussed below.

Table 1. Experimentally and Theoretically Determined Values (in eV) of Adiabatic Electron Affinities (EA_a), Vertical Detachment Energies (VDE), and HOMO−LUMO Gaps for $Al_4H_m^-$ ($m = 4, 6$) and $Al_nH_{n+2}^-$ ($5 \leq n \leq 8$).

	EA_a		VDE		HOMO–LUMO gap	
	experiment	theory	experiment	theory	experiment	theory
Al_4H_4	$1.35^a \pm 0.05$	1.45	$1.65^a \pm 0.05$	1.71	$1.55^a \pm 0.15$	1.36
Al_4H_6	1.25 ± 0.15	1.36	1.35 ± 0.05	1.48	1.9 ± 0.1	1.85
Al_5H_7	1.9 ± 0.1	2.11	2.20 ± 0.05	2.18	0.95 ± 0.10	0.87
Al_6H_8	2.4 ± 0.3	2.17	2.65 ± 0.05	2.70	0.6 ± 0.1	0.51
Al_7D_9	2.2 ± 0.2	2.17	2.6 ± 0.1	2.87	0.8 ± 0.15	0.58
Al_8H_{10}	2.3 ± 0.2	1.94	2.8 ± 0.1	2.79	1.0 ± 0.2	1.14

[a] Values for the ground state anion (isomer A).

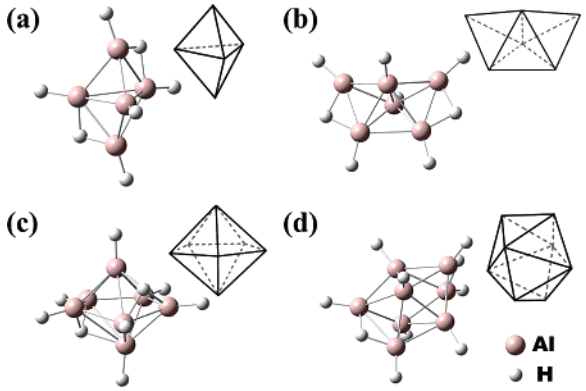

Figure 4. Calculated ground state structures of Al_nH_{n+2} ($5 \leq n \leq 8$) clusters: (a) Al_5H_7; (b) Al_6H_8; (c) Al_7H_9; (d) Al_8H_{10}. Solid figures to the side of each cluster represent the aluminum cages idealized (undistorted) polyhedral structure.

3.1.2. Hexaalane ($n + 2 = 8$): Al_6H_8. The photoelectron spectrum of $Al_6H_8^-$ (Figure 2) displays two major peaks on the low EBE side of the spectrum (2.65 ± 0.05 and 3.25 ± 0.05 eV) and a broad featureless region of transitions stretching to the higher binding energies. Its substantial HOMO−LUMO gap (0.6 ± 0.1 eV) and small EA_a value (2.4 ± 0.3 eV) relative to most of the remaining members of Al_6H_m series (Figure 3b) again portrays the Al_nH_{n+2} stoichiometry as among the most stable ones. The long tail on the low EBE side of the origin peak made it difficult to assign a more accurate value of EA_a. Our calculated value of EA_a is 2.17 eV. All measured and calculated quantities are summarized in Table 1.

Consistency between theoretically predicted values and those extracted from the photoelectron spectrum of $Al_6H_8^-$ again gave credibility to computationally derived conclusions about the corresponding neutral. Its ground state structure, shown in Figure 4b, is that of a bicapped tetrahedral Al_6H_6 core with two bridging hydrogen atoms occupying opposite edges of the framework, again in agreement with Wade's predictions for the closo-systems. Although, octahedral skeletal arrangement is the preferred choice according to the Wade's rules in case of boranes, the more compact geometry of a bicapped tetrahedron

is often adopted by metal core-containing clusters (i.e., $Os_6(CO)_{18}$).[30] A similar tendency in the case of aluminum not only reflects its ability to access the 3d-orbitals (in excitation) that boron lacks, but also its embryonic metallic character that will come to dominate in larger clusters. Note that the bicapped tetrahedron is a 6-vertex polyhedron, too, and consequently represents one of the possible structures predicted by the Wade's ($n + 1$) rule. There may also be a relation to $Al_6R_6^-$, the only preparatively obtained distorted octahedron known in aluminum chemistry.[31]

3.1.3. Heptaalane ($n + 2 = 9$): $Al_7H_9^-$. Here, in Figure 2, we present the photoelectron spectrum of $Al_7D_9^-$ in place of $Al_7H_9^-$, since the spectrum of the latter was of poorer quality than that of the former. Aside from a lower signal-to-noise ratio in the case of $Al_7H_9^-$, the two spectra were essentially the same. A substantial HOMO−LUMO gap (0.80 ± 0.15 eV) is observed between the two lowest features of the $Al_7D_9^-$ spectrum, that is, 2.6 ± 0.1 and 3.40 ± 0.05 eV. We estimate the EA_a value of Al_7D_9 to be 2.2 ± 0.2 eV. There are at least two more transitions at higher EBEs (3.85 ± 0.15, 4.2 ± 0.1 eV). A plot of EA_a values and HOMO−LUMO gaps across the Al_7H_m series (see Figure 3c) again reveals enhanced stability for the species with stoichiometry Al_nH_{n+2} relative to its neighbors. [The origin of the stability of Al_7H (shows the largest HOMO−LUMO gap in the series) can be understood in terms of the shell model, and this will be discussed in a separate publication.]

The theoretical results given in Table 1 are consistent with the experimental results and give confidence in deductions about neutral Al_7D_9 and therefore about Al_7H_9. Its ground state structure, shown in Figure 4c is a pentagonal bipyramidal Al_7H_7 cage with two facile hydrogen atoms, consistent with the expectations of the Wade's ($n + 1$) rule. It is interesting to note that unlike the hexaalane, Al_7H_9 does not adopt a more compact capped structure, such as the capped octahedral arrangement found for $Os_7(CO)_{21}$,[32] thereby emphasizing the importance of considering all possible structures of species in the small cluster regime.

3.1.4. Octaalane ($n + 2 = 10$): Al_8H_{10}. The photoelectron spectrum of $Al_8H_{10}^-$, shown in Figure 2, displays only two distinct peaks (2.8 ± 0.1, 4.1 ± 0.1 eV) with a shoulder at 3.8 $\pm$ 0.1 eV. The HOMO−LUMO gap was estimated to be 1.0 ± 0.2 eV from the separation between the first peak and the shoulder at 3.8 eV. Comparing HOMO−LUMO gaps and EA_a values among the other members of the $Al_8H_m^-$ series presented in Figure 3d shows that several other stoichiometries in addition to Al_nH_{n+2} also exhibit heightened HOMO−LUMO gaps and reduced EA_a values. Thus, its special position among its neighbors is not as strong as in the systems previously described. Nevertheless, the large HOMO−LUMO gap and low EA_a (2.3 ± 0.2 eV) of Al_8H_{10} implies that it is a cluster with enhanced stability.

The theoretically determined values for EA_a (1.94 eV), VDE (2.79 eV), and the HOMO−LUMO gap (1.14 eV) of the ground-state structure are in good agreement with the observed spectral features, adding confidence in the theoretical conclusions. The ground state isomer is found to adopt a polyhedral Al_8H_8 core with two bridging hydrogen atoms located on opposite edges in agreement with the Wade's ($n + 1$) rule. A similar structure is observed for boranes, whereas in transition metal-core clusters, such as $[Os_8(CO)_{22}]^{2-}$, alternative 8-vertex polyhedral arrangements are often encountered.[33] Not only does this make aluminum more of a main group element than a metal in the alanes of this size regime but also supports our contention that the studied alanes can be considered as borane analogues.

3.1.5. $Al_nH_n^{2-}$ Speculation. Closo-borane dianions, $B_nH_n^{2-}$, are among the most stable borane species known, serving as paramount examples for the success of the Wade's ($n + 1$) rule. Yet the corresponding diprotonated species B_nH_{n+2} have so far avoided detection. Our observation of substantial HOMO−LUMO gaps for Al_nH_{n+2} species implies their enhanced stabilities and naturally raises questions about the possible existence of deprotonated closo-alanates, $Al_nH_n^{2-}$. Since the ion sources employed in our gas-phase cluster studies generally do not produce appreciable amounts of doubly charged anions, direct evidence is not available. However, singly charged, monoprotonated species, $Al_nH_{n+1}^-$, are readily made. Formally written as $Al_nH_n^{2-} + H^+$, these clusters should be closed-shell species with a tightly bound excess electron. High values of EA_a for Al_nH_{n+1} ($5 \leq n \leq 8$) species (see Figure 3) are consistent with this picture. This is seen for Al_5H_6 in the Al_5H_m series (see Figure 3), for Al_6H_7 in the Al_6H_m series, for Al_7H_8 in the Al_7H_m series, and strongly for Al_8H_9 in the Al_8H_m series. In some cases this observation is muted by the gradual rise in EA_a values with increasing cluster size, but in every case, the Al_nH_{n+1} species has the highest EA_a in its series, albeit marginally so in some cases. We therefore speculate that the closo-alanates of general formula $Al_nH_n^{2-}$ have the potential to exist in direct analogy with the known closo-boranates, $B_nH_n^{2-}$. Indeed, the reported synthesis of a material containing $(Al_{12}R_{12})^{2-}$ supports this speculation.[34]

3.2. $Al_4H_m^-$ Series. The photoelectron spectra of the $Al_4H_m^-$ series ($3 \leq m \leq 7$) are presented in Figure 5, and a plot of EA_a and HOMO−LUMO gap values versus m for the $Al_4H_m^-$ series is shown in Figure 6. Relatively high HOMO−LUMO gaps and low EA_a values, compared to those of their neighbors, are evident for two species, Al_4H_4 and Al_4H_6. The special status of the $n = 4$ case in PSEPT led us to dedicate a separate section for the discussion of these systems.

The application of PSEPT concepts to the case of $n = 4$ generates an energy level diagram schematically shown in Figure 7. In Figure 7 (left), which is pertinent to T_d symmetry, HOMO−LUMO gaps can emerge for structures containing either four or six skeletal electron pairs.[17,25] Here, the reason for the tetrahedral exception to Wade's ($n + 1$) electron rule becomes clear. Five electron pairs would imply $n = 4$ and thus seemingly to T_d symmetry, but this would actually lead to two, singly occupied degenerate e_g orbitals and thus to Jahn−Teller distortion of the tetrahedral structure. If, however, the symmetry is reduced to D_{2d}, the topmost set of orbitals splits [see Figure 7 (right)], and, depending on the extent of departure from T_d symmetry, the ($n + 1$) rule can be rehabilitated. Thus, the interplay of environmental symmetry effects and the available

(30) Blake, A. J.; Johnson, B. F. G.; Nairn, J. G. M. *Acta Crystallogr., Sect. C* **1994**, *50*, 1052.
(31) Dohmeier, M.; Mocker, H.; Schnöckel, H.; Lötz, A.; Schneider. U.; Ahlichs. R. *Angew. Chem.* **1993**, *105*, 1491.
(32) Eady, C. R.; Johnson, B. F. G.; Lewis, J.; Mason, R.; Hitchcock, P. B.; Thomas, K. M. *J. Chem. Soc., Chem. Commun.* **1977**, 385.
(33) Jackson, P. F.; Johnson, B. F. G.; Lewis, J.; Raithby, P. R. *J. Chem. Soc., Chem. Commun.* **1980**, (2), 60.
(34) Hiller, W.; Klinkhammer, K.-W.; Uhl, W.; Wagner, J. *Angew. Chem., Int. Ed. Engl.* **1991**, *30*, 179.

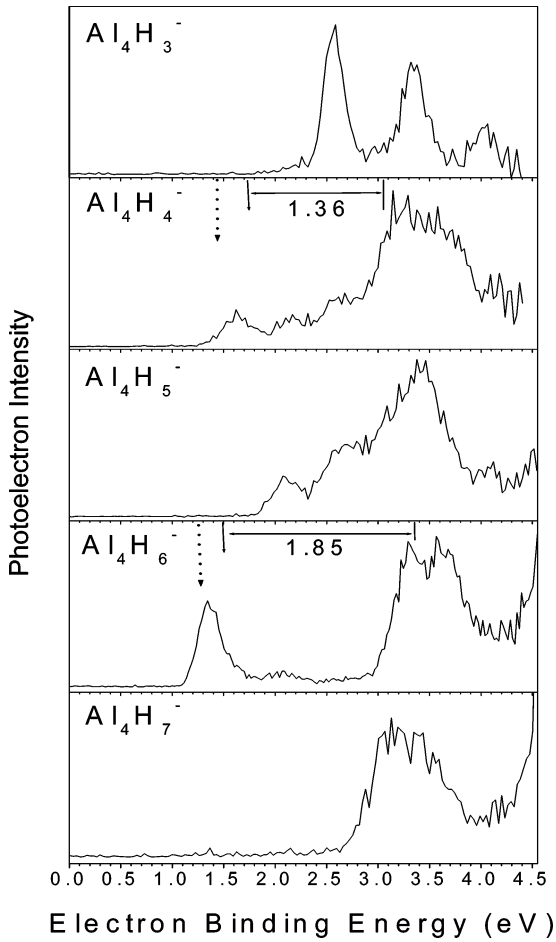

Figure 5. Photoelectron spectra of $Al_4H_m^-$ series ($3 \le m \le 7$) recorded with 4.661 eV photons. Arrows indicate theoretically calculated values for EA_a (dotted, vertical), VDE (solid, vertical), and HOMO−LUMO gaps (solid, horizontal) of $Al_4H_4^-$ and $Al_4H_6^-$.

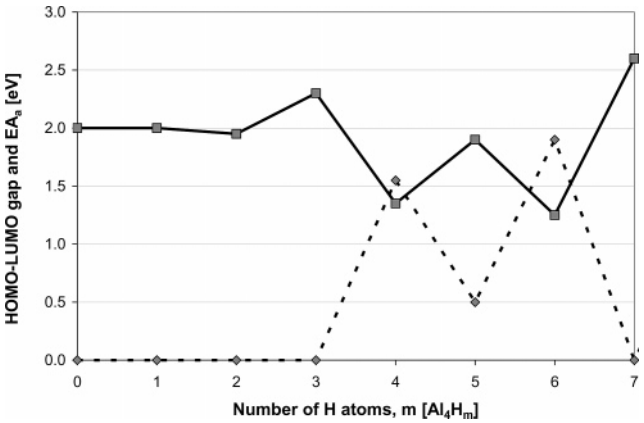

Figure 6. HOMO−LUMO gaps (dashed) and EA_a values (solid lines) for clusters of the Al_4H_m series versus the number of hydrogen atoms, *m*. Data are extracted from photoelectron spectra shown in Figure 5.

number of skeletal electron pairs may account for the observed structural diversity of B_4[35] and Al_4[23,24,36−39] cores. In what

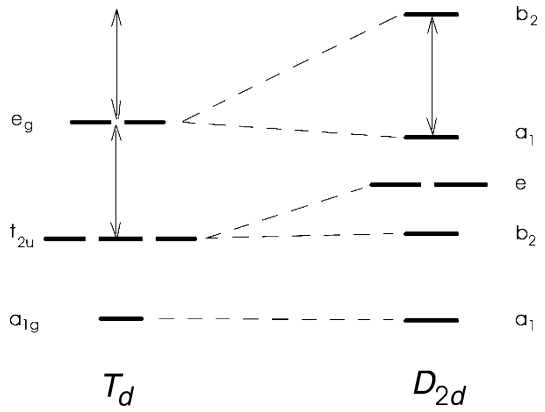

Figure 7. Bonding molecular orbital diagram for a T_d (left) and D_{2d} (right) symmetric four-vertex polyhedral framework (such as Al_4H_4), derived from PSEP theory. Arrows indicate the most likely location of large energy gaps and reveal that to stabilize a framework of T_d symmetry either four or six skeletal electron pairs are required, whereas five of them are needed to stabilize a D_{2d} cage. The figure depicts the molecular orbital reasons for the known exception to the Wade's ($n + 1$) rule in the case of T_d symmetry and the reinstatement of the ($n + 1$) rule when D_{2d} symmetry is adopted.

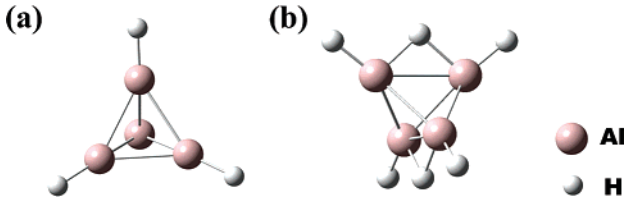

Figure 8. Calculated neutral ground state structures of (a) Al_4H_4 and (b) Al_4H_6.

follows, the observed structures of both Al_4H_4 and Al_4H_6 are discussed in terms of the fundamental PSEPT concepts, since the Wade's ($n + 1$) rule does not strictly apply to these closo-systems.

3.2.1. Tetraalane ($m = 4$): Al_4H_4. The photoelectron spectrum of $Al_4H_4^-$ shows at least five transitions (1.65 ± 0.05, 2.10 ± 0.05, 2.6 ± 0.1, 3.2 ± 0.1, 3.65 ± 0.10 eV). Changing the conditions in the source caused shifts in relative peak heights indicating a presence of isomers. Two groups of peaks were identified and attributed to isomers A (1.65 ± 0.05, 3.2 ± 0.1) and B (2.10 ± 0.05, 2.6 ± 0.1, 3.2 ± 0.1, 3.65 ± 0.10 eV). The relative intensities of these features suggest that isomer A is the more abundant of the two. Theoretical calculations found isomer A to be the ground state. Its calculated EA_a is 1.45 eV, its calculated VDE is 1.71 eV, and its calculated HOMO−LUMO gap is 1.36 eV. These all agree well with the experimentally determined values summarized in Table 1.

The calculated geometry of the neutral ground state is given in Figure 8a. The structure adopts T_d symmetry with four aluminum atoms located in corners of a perfect tetrahedron and four hydrogen atoms occupying terminal sites on each aluminum atom. The calculated molecular orbital diagram shows a large energy gap emerging above the four bonding skeletal orbitals. This diagram is analogous to the PSEPT-derived schematic diagram depicted in Figure 7 (left). With four electron pairs available to occupy the available bonding orbitals of the aluminum skeleton, the observed structure is in agreement with the expectations of the PSEP theory for T_d symmetry. It is also worth noting that both Al_4R_4[23,24] and B_4R_4 (R = ^{t}Bu, $CH_2{}^t$Bu, Cl, Br)[25] have been synthesized in the crystalline state. They all adopt tetrahedral geometries. In addition, calculations have

(35) Schnöckel, H. *Dalton Trans.* **2005**, *19*, 3131.
(36) Dohmeier, C.; Loos, D.; Schnöckel, H. *Angew. Chem., Ed. Int. Engl.* **1996**, *35* (2), 129.
(37) Li, X.; Kuznetsov, A. E.; Zhang, H. F.; Boldyrev, A. I.; Wang, L.-S. *Science* **2001**, *291*, 859.
(38) Linti, G.; Schnöckel, H.; Uhl, W.; Wiberg, N. *Molecular Clusters of the Main Group Elements*; Wiley-VCH: Weinheim, Germany, 2002.
(39) Schnepf, A.; Schnöckel, H. *Angew. Chem., Ed. Int.* **2002**, *41* (19), 3533.

been published about the structure and bonding of $Al_4R_4^-$, where $R = Si(SiMe_3)_3$.[40]

3.2.2. Tetraalane ($m = 6$): Al_4H_6. Al_4H_6 has a relatively low EA_a (1.25 ± 0.15 eV) and the largest HOMO−LUMO gap (1.9 ± 0.1 eV) of any $Al_nH_m^-$ system that we studied. This implied extraordinary stability motivated us in a previous publication to use Al_4H_6 as a first example for introducing this new chapter in aluminum hydride chemistry.[29] Here, we describe reasons for its stability in greater detail.

Having the same general formula Al_nH_{n+2} as previously discussed closo-alanes, we intentionally avoided putting them into the same category. Namely, treating Al_4H_6 as hypothetical $Al_4H_4^{2-} + 2H^+$ and invoking Wade's $(n + 1)$ rule (as we did with the other systems) fails here, because five skeletal electron pairs only half-fill the upper most shell.[25] This scenario is not consistent with the observed highly stable and slightly distorted tetrahedral, D_{2d} structure depicted in Figure 8b. While considering the two H^+ ions only as bystanders in Al_nH_{n+2} systems, where $n > 4$, those two bridging protons are of utmost importance in $n = 4$ case. Namely, they cause an inherent decrease of symmetry of the cluster leading to the PSEPT-derived energy-level diagram schematically shown in Figure 7 (right) for D_{2d} symmetry. In addition, positive charge from the two protons stabilizes the lower of the two topmost orbitals further increasing the splitting. Theoretical calculations on Al_4H_6 support this picture by revealing five bonding orbitals below a substantial gap in energy levels. Al_4H_6 serves as a poignant reminder that while the Wade's rules are a great guide for explaining geometries of many cluster compounds, it is the underlying PSEPT or the Wade−Mingos rules that ultimately determine the structure adopted by the cluster.

4. Conclusions

Through a combination of anion photoelectron spectroscopy and theoretical computations several previously unknown aluminum hydrides were studied. High HOMO−LUMO gaps and relatively low EA_a values observed for Al_4H_4, Al_4H_6, and the family, Al_nH_{n+2} $(5 \leq n \leq 8)$ indicate that they possess substantial stability over their stoichiometric neighbors. Similarity with the formulas of known boranes prompted us to investigate whether Wade's rules could be applied to these alanes. The correspondence of EA_a, VDE, and HOMO−LUMO gap values derived from DFT calculations with those extracted from measured photoelectron spectra of $Al_nH_m^-$ species allowed us to deduce the geometries of the neutral Al_nH_m species.

The Al_nH_{n+2} $(5 \leq n \leq 8)$ family was shown to adopt closo-structures with two extra hydrogen atoms occupying bridging positions in agreement with the Wade's $(n + 1)$ rule. Al_4H_4 was found to assume a closo-tetrahedral cage. Al_4H_6 takes on a distorted tetrahedral (D_{2d}) structure with two bridging hydrogen atoms and shows the largest HOMO−LUMO gap (1.9 ± 0.1 eV) of all studied alanes.[29] This seeming contradiction with the predictions of the tetrahedral exception to the Wade's $(n + 1)$ rule can be understood in terms of the underlying PSEPT concept. Applying these concepts to D_{2d} symmetry gives rise to an energy-level diagram, where the topmost, degenerate set of e_g bonding orbitals (in T_d symmetry) split. This creates a HOMO−LUMO gap between these fifth and sixth skeletal bonding orbitals, such that a ten electron system, such as Al_4H_6, adopts a distorted tetrahedral structure and becomes stable. Consequently, the Wade's $(n + 1)$ rule can be extended to include the $n = 4$ cases of D_{2d} symmetry. The ability to understand the observed alanes with enhanced stability in terms of the Wade's rules or the underlying PSEPT concept suggests that they can be considered as borane analogues, opening a new chapter in aluminum hydride chemistry.

Whether these species can be synthesized in macroscopic quantities remains to be seen. While they are presumably metastable relative to the ultimate thermodynamic minimum of aluminum metal and hydrogen gas phases, there may be sufficiently high barriers in their dissociation channels such that they could be synthesized. If so, these compounds would not only release their binding energies to produce the aluminum metal and hydrogen, but upon reaction with oxygen, huge amounts of energy, associated with their combustion to Al_2O_3 and H_2O, would also be released.

Acknowledgment. K.B. thanks the Air Force Office of Scientific Research for its support of this work. P.J. thanks the Office of Basic Energy Sciences, Department of Energy. Both G.G. and H.S. acknowledge the Deutsche Forschungsgemeinschaft.

Supporting Information Available: Complete ref 28; coordinates and energies of calculated neutral structures. This material is available free of charge via the Internet at http://pubs.acs.org.

JA0700404

(40) Vollet. J.; Stösser, H.; Schnöckel, H. *Inorg. Chim. Acta* **2007**, *360* (4), 1298.